Nitrile *N*-Selenide (RC≡NSe) and Isoselenocyanate (RN=C=Se) Neutrals and Radical Cations by Selenation of Nitriles and Isonitriles: Tandem Mass Spectrometry and ab Initio Studies

Pascal Gerbaux,[†] Robert Flammang,*[,†] Eva H. Mørkved,[‡] Ming Wah Wong,*[,§] and Curt Wentrup[||]

Organic Chemistry Laboratory, University of Mons-Hainaut, B-7000 Mons, Belgium, Department of Organic Chemistry, Norwegian University of Sciences and Technology, N-7034 Trondheim, Norway, Department of Chemistry, National University of Singapore, 119260 Kent Ridge, Singapore, and Department of Chemistry, The University of Queensland, Brisbane, QLD 4072, Australia

Received: June 2, 1998

Cyanogen *N*-selenide radical cations, $NCCNSe^{\bullet+}$ (**4**$^{\bullet+}$), have been produced by dissociative ionization of 3,4-dicyano-1,2,5-selenadiazole (**3**). By using a new hybrid tandem mass spectrometer, it is shown that these ions are excellent agents of selenation of nitriles and isonitriles, producing nitrile *N*-selenide ions ($RCNSe^{\bullet+}$) and isoselenocyanate ions ($RNCSe^{\bullet+}$), respectively. The connectivities of these ions have been established by collisional activation, and the stabilities of the corresponding neutrals were probed by neutralization−reionization experiments and ab initio G2(MP2,SVP) calculations. The neutral nitrile *N*-selenides are found by experiment and theory to be observable species in the gas phase. All the cations are potential energy minima, and their calculated fragmentation energies are in accord with experimental observations. $NCCNSe^{\bullet+}$ is found to be an effective $Se^{\bullet+}$ transfer agent because of its low N−Se bond dissociation energy and exceptional low-lying LUMO. The effect of substituents (CH_3, NH_2, OH, F, Cl, Br, I, CN, and SCH_3) on the structures and stabilities of RCNSe neutrals is also reported.

Introduction

1,3-Dipolar cycloadditions are widely used in heterocyclic chemistry[1] and, among a large variety of 1,3-dipoles, particular attention has been paid to nitrilium betaines (R−C≡N$^+$−X$^-$).[2] For instance, nitrile oxides (R−C≡N−O) have played an important role in the development of chemistry. The early known representatives of this family are the fulminic acid salts (Ag and Hg fulminates) discovered by the alchemists and used as explosives. In 1824, the first experimental evidence for isomerism stemmed from the realization by Liebig and Wöhler, respectively,[3] that the salts of fulminic acid, HCNO,[3a] and isocyanic acid, HNCO,[3b] have the same elementary composition but are structurally distinct.[4] Nitrile oxides are easily produced from readily accessible precursors such as furoxans (thermolysis),[5] dihaloformoximes (photolysis),[6] or cyanoformhydroximic chloride (reaction with aqueous base).[7] Moreover, dissociative ionization of furoxans or furazans in the gas phase of a mass spectrometer generates nitrile oxide radical cations.[8]

Nitrile imines[9] (R−C≡N−NR′) and nitrile ylides (R−C≡N−CR′$_2$), although less frequently described in the literature, are nevertheless readily generated.[1,2] Recently, the unsubstituted formonitrile imine (HCNNH) has been isolated both in the gas phase[10] and in a matrix.[11] The unsubstituted formonitrile ylide, $HCNCH_2$, has been detected by mass spectrometry methodologies and also by matrix-isolation IR spectroscopy.[12] Nitrile ylide radical cations are readily generated by transfer of $CH_2^{\bullet+}$ from distonic ions such as $^{\bullet}CH_2OCH_2^+$ (ionized oxirane)[13] or $^{\bullet}CH_2CH_2CO^+$ (ionized cyclobutanone)[13] to neutral nitriles in a mass spectrometer.[14]

Although extremely unstable and short-lived species under usual reaction conditions, nitrile sulfides (R−C≡N−S) have been known as reactive intermediates for 25 years[15] and their definitive spectroscopic characterization was achieved more recently.[16] Most of the precursors of these reactive species are five-membered heterocyclic compounds incorporating at least one CNS linkage.[15,16] In addition to these previous works, it has been shown that nitrile sulfide radical cations are efficiently generated by electron ionization of 1,2,5-thiadiazoles.[17] Collision-induced neutralization of nitrile sulfide radical cations, the first step of the neutralization−reionization methodology,[18] has allowed the production of the neutral sulfides in the gas phase.[17] It was also found that $CS_3^{\bullet+}$ radical cations, produced by chemical ionization (self-CI) of carbon disulfide, react readily with nitriles, leading to the corresponding nitrile sulfide radical cations with good yield.[19]

Much less is known about nitrile selenides (R−C≡N−Se). There is good evidence[20] for their existence at low temperature (<100 K), but attempts to trap them with dipolarophiles have failed so far. The approach used to detect these short-lived species was very similar to that successfully employed for isolating and studying nitrile sulfides. On photolysis of 3,4-diphenyl-1,2,5-selenadiazole (**1**) at 85 K in a PVC film, a transient was observed with λ_{max} at 255, 325, 360 and 390 nm. On heating above 100 K or irradiation (300 or 360 nm), selenium was deposited and signals attributed to benzonitrile selenide (**2**) were replaced by those of benzonitrile (Scheme 1). Consequently, the thermal and photochemical behaviors of nitrile selenides and sulfides are similar. Indeed, photolysis of

[†] University of Mons-Hainaut.
[‡] Norwegian University of Sciences and Technology.
[§] National University of Singapore.
[||] The University of Queensland.

10.1021/jp9824454 CCC: $15.00
Published on Web 10/17/1998

SCHEME 1

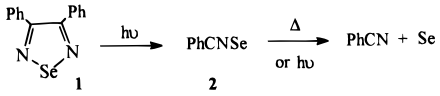

SCHEME 2

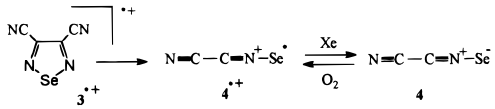

nitrile sulfides at cryogenic temperatures or allowing the sample to warm above 100 K results in desulfuration.[21] In contrast, the nitrile oxides rearrange upon photolysis to the isomeric isocyanates, with oxazirenes and acylnitrenes as likely intermediates.[6,22] The failure of trapping reactions, even with a reactive dipolarophile, can be attributed to the fact that nitrile selenides are less stable and more prone to fragmentation than the corresponding oxides and sulfides.

In the present work, we report on the generation and the characterization of nitrile *N*-selenides (RC≡NSe) as neutrals and radical cations in the gas phase of a mass spectrometer. High-level ab initio calculations were also performed in an effort to understand the structures and stabilities of this new class of molecules.

Results and Discussion

Following 70 eV electron ionization, 3,4-dicyano-1,2,5-selenadiazole (**3**$^{\bullet+}$) was shown to lose predominantly cyanogen, leading to cyanogen *N*-selenide radical cations (**4**$^{\bullet+}$) (Scheme 2).[23] The NCCNSe connectivity of these *m*/*z* 132 ions (^{80}Se-containing ions) was deduced from the collisional activation (CA) spectrum, and the stability of the corresponding neutral dipoles in the gas phase was established by a neutralization−reionization experiment (NRMS). The NR spectrum featured indeed a weak but significant recovery signal corresponding to "survivor" ions and fragmentations similar to those observed in the CA spectrum.

The NCCNSe dipole was an unknown member of the NCCNX family.[24] Westwood *et al.* have extensively described the generation and the characterization of cyanogen *N*-oxide,[5b,c,25] while our groups have reported on the production of the corresponding cyanogen *N*-sulfide.[17]

Neutral cyanogen *N*-selenide (**4**) is calculated to be stable with respect to all possible fragmentation processes (section 5), and this is corroborated by the NR mass spectrum featuring an intense recovery signal for survivor ions. Consistent with the experimental observations, cyanogen *N*-selenide radical cations (**4**$^{\bullet+}$) are also predicted to be stable with respect to simple cleavage fragmentations. The calculated fragmentation energies (section 5) of **4**$^{\bullet+}$ agree with the observed CA spectrum.[23] Formation of Se$^{\bullet+}$ (*m*/*z* 80) is the most favorable fragmentation process. NCCNS$^{\bullet+}$ ions also predominantly decompose by S$^{\bullet+}$ formation after collisional activation[17] while NCCNO$^{\bullet+}$ ions predominantly lose NCC$^{\bullet}$ to generate NO^{+} ions.[8]

In a previous report,[23] it was also shown that the decreasing intensity of the recovery signals in the NR spectra of the NCCNX series (X = O, S, and Se) was in keeping with theoretical calculations: the energy requirement for the dissociation into NCCN + X decreases with the electronegativity of X. It was calculated, at the G2(MP2,SVP) level of theory, that the endothermicities of the reactions NCCNX → NCCN + X follow the sequence O > S > Se, being 415, 244, and 187 kJ mol^{-1}, respectively.

TABLE 1: EI (70 eV) and Self-CI Mass Spectra of 3,4-Dicyano-1,2,5-selenadiazole (3)

electron ionization		self-chemical ionization		
m/*z*[a]	relative abundance (%)	*m*/*z*[a]	relative abundance (%)	structure
38	30	38	14	CCN^{+}
52	78	52	34	$NCCN^{\bullet+}$
80	96	80	92	$Se^{\bullet+}$
106	10	106	10	$CNSe^{+}$
132	100	132	100	$NCCNSe^{\bullet+}$ (**4**$^{\bullet+}$)
184	72	184	98	**3**$^{\bullet+}$
		264	24	[**3** + Se]$^{\bullet+}$

[a] Masses indicated for the ^{80}Se-containing ions.

SCHEME 3

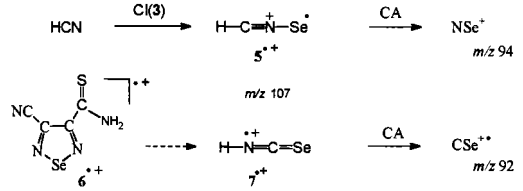

1. Self-Chemical Ionization of 3. When 3,4-dicyano-1,2,5-selenadiazole (**3**) is ionized in a gastight ion source at an estimated pressure of approximately 0.5−1 Torr (self-CI conditions), ions similar to those observed with pure EI conditions are produced (Table 1). The main difference is the observation of *m*/*z* 264 radical cations in the former case, ions generated by an ion−molecule reaction transferring Se$^{\bullet+}$ ions to **3**. The actual structure of these ions cannot be deduced easily by collisional activation [CA *m*/*z* (%): 212 (10), 184 (8), 160 (82), 132 (36), 106 (20), 80 (100)]. The selenadiazole ring seems to be preserved, but the possible location of the added Se$^{\bullet+}$ on either a ring nitrogen, a nitrogen atom of a nitrile group, or the ring selenium cannot be determined by the present experiment alone, as a very intense peak at *m*/*z* 160 ($Se_2^{\bullet+}$) is notable. Whatever the site of selenation of **3**, the main result of this experiment is the fact that ions derived from the ionization of **3** are able to transfer selenium to functional groups in other molecules. In the following experiments, we have chosen nitriles as the potential targets for selenation.

2. Se$^{\bullet+}$ Transfer to Nitriles. Chemical ionization of hydrogen cyanide (HCN) using 3,4-dicyano-1,2,5-selenadiazole (**3**) as the reagent gas leads to the formation of [HCN,Se]$^{\bullet+}$ ions (*m*/*z* 107). The connectivity of these ions has been previously studied by collisional activation experiments (Figure 1a), and the HCNSe connectivity (**5**) has been unambiguously confirmed.[23] In particular, the observation of a peak at *m*/*z* 94 (loss of CH) is worthy of note (Scheme 3). The calculated fragmentation pattern of **5**$^{\bullet+}$ agrees quite well with the relative intensities in the CA spectrum (section 5). The formation of Se$^{\bullet+}$ ions is the energetically most favorable fragmentation.

Further support for the HCNSe structure (**5**) is found in the study of another selenadiazole (**6**). Indeed, the dissociative ionization of **6** also generates [H,C,N,Se]$^{\bullet+}$ ions through a reaction sequence involving probably a [1,4] hydrogen transfer on the ring nitrogen and the losses of HNCS and cyanogen. The CA spectrum of these *m*/*z* 107 ions (Figure 1b), although dominated by a very intense peak corresponding to selenium ions, features a significant and very characteristic peak when compared to the CA spectrum of **5**$^{\bullet+}$ ions produced by Se$^{\bullet+}$ transfer to HCN (Figure 1a): the loss of HC (*m*/*z* 94, NSe^{+}) observed in the case of **5**$^{\bullet+}$ ions is replaced by a loss of HN (*m*/*z* 92, $CSe^{\bullet+}$) indicative of the isoselenocyanate structure (**7**)

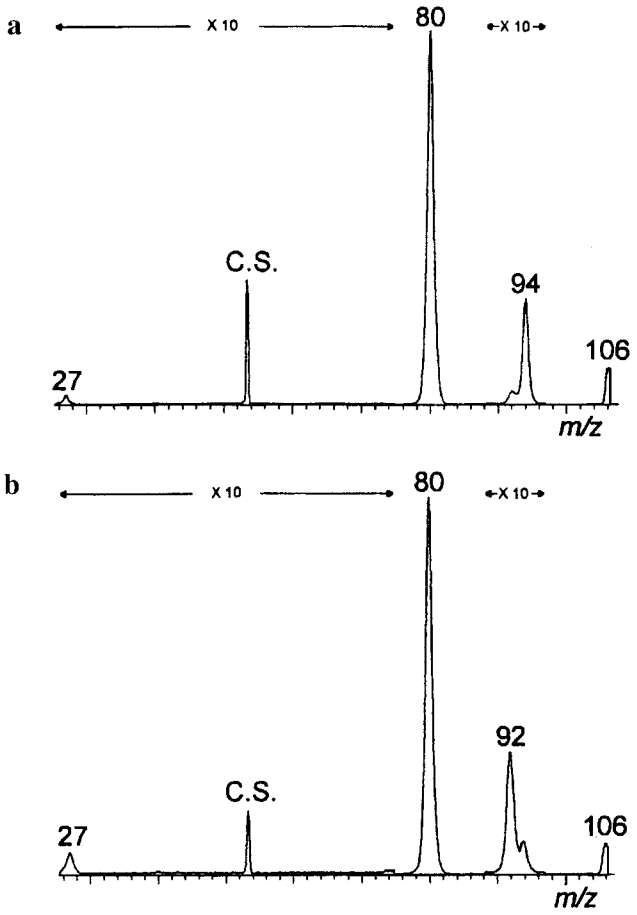

Figure 1. (a) CA (O_2) mass spectrum of the *m*/*z* 107 ions[23] ($HCNSe^{\bullet+}$) generated by $Se^{\bullet+}$ transfer to HCN under CI conditions. (b) CA (O_2) mass spectrum of the *m*/*z* 107 ions ($HNCSe^{\bullet+}$) produced by dissociative ionization of 4-cyano-1,2,5-selenadiazole-3-carbothioamide (**6**) (C.S. = charge stripping).

(Scheme 3). $HCNSe^{\bullet+}$ (**5**$^{\bullet+}$) and $HNCSe^{\bullet+}$ (**7**$^{\bullet+}$) ions therefore show the same behavior as their sulfur analogues; the CA spectra of $HCNS^{\bullet+}$ and $HNCS^{\bullet+}$ ions can also be distinguished by means of the [M − HC]/[M − HN] ratios.[19]

Significant recovery signals are present in the NR spectra of the $HCNSe^{\bullet+}$ (**5**$^{\bullet+}$) and $HNCSe^{\bullet+}$ (**7**$^{\bullet+}$) radical cations; it is concluded that the neutral HCNSe and HNCSe molecules are stable and distinct molecules in the gas phase. Neutral HCNSe (**5**) is calculated to be stable with respect to all possible unimolecular fragmentation processes (section 5). Loss of Se atom and loss of H are the most favorable dissociation pathways. Hence, neutral HCNSe is confirmed as an experimentally accessible and intrinsically stable species in the gas phase.

$[CH_3CN,Se]^{\bullet+}$ ions (*m*/*z* 121) are also readily generated during the chemical ionization of acetonitrile using dicyanoselenadiazole **3** as the reagent gas. After collisional activation (Figure 2a), these ions predominantly lose neutral acetonitrile, generating $Se^{\bullet+}$ ions (*m*/*z* 80). This behavior is clearly in keeping with the relevant ionization energies given in Table 2.[26] Likewise, the less intense peaks at *m*/*z* 106 (loss of $CH_3^{\bullet}$) and at *m*/*z* 94 (loss of $CH_3C^{\bullet}$) are also indicative of the acetonitrile *N*-selenide connectivity (**8**) (Scheme 4, R = CH_3). The peak at *m*/*z* 93 (loss of CH_2N) must arise from a rearrangement process (this is further discussed in the context of the NR spectra of **8** and **9**; see below). Again these experimental data are in keeping with the calculated fragmentation energies (section 5), except for the signal corresponding to the loss of H$^{\bullet}$, which is predicted by theory to be intense.

TABLE 2: Relevant Ionization Energies[a] and $Se^{\bullet+}$/$RCN^{\bullet+}$ Abundance Ratios in the CA Spectra of the RCNSe or RNCSe Radical Cations

neutral	ionization energy (eV)	$Se^{\bullet+}$/RCN $(RNC)^{\bullet+}$
HCN	13.6	305
HNC	12.5	170
ClCN	12.34	13
CH_3CN	12.2	50
BrCN	11.84	
CH_3NC	11.24	20
ICN	10.87	1.7
CH_3SCN	9.96	3.5
Se	9.75	-
PhCN	9.62	0.2
PhNC	9.4	0.5

[a] From ref 26.

SCHEME 4

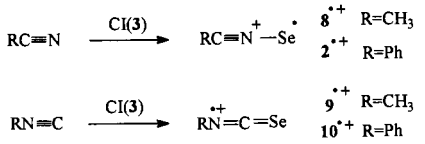

During the study of the analogous sulfur transfer to acetonitrile,[19] the *N*-sulfide connectivity was definitely confirmed by comparing the collision-induced fragmentations of $CH_3CNS^{\bullet+}$ radical cations with those of the molecular ions of methyl isothiocyanate, $CH_3NCS^{\bullet+}$. Although several methods for the preparation of alkyl isoselenocyanate have been investigated in the literature,[27a−e] methyl isoselenocyanate (**9**) is not commercially available. However, it is known that $CH_2^{\bullet+}$ is easily transferred from ionized cyclobutanone to methyl isocyanide (CH_3NC) to produce methyl ketenimine radical cations ($CH_3NCCH_2^{\bullet+}$) in the gas phase.[28] Similarly, $S^{\bullet+}$ transfer (from $CS_3^{\bullet+}$ ions) efficiently generates $CH_3N{=}C{=}S^{\bullet+}$ ions.[29] These observations prompted us to try the chemical ionization of CH_3NC with dicyanoselenadiazole **3** as the CI gas. In this way, $[CH_3NC,Se]^{\bullet+}$ ions are indeed produced in high yield (Scheme 4, R = CH_3). The CA spectrum of these ions (Figure 2b) is not very different from the CA spectrum of the $CH_3CNSe^{\bullet+}$ ions (**8**$^{\bullet+}$); nevertheless, significant differences are seen at *m*/*z* 92 (loss of CH_3N) and in the region corresponding to doubly charged ions (charge stripping, C.S.). In fact, in contrast to the case of the $CH_3CNSe^{\bullet+}$ ions (**8**$^{\bullet+}$), a significant signal corresponding to C_2HNSe^{2+} cations is present in the CA spectrum of the $CH_3NCSe^{\bullet+}$ ions (**9**$^{\bullet+}$). This peculiar behavior is not unexpected, as the loss of 2H (H_2) from the doubly charged CH_3NCX^{2+} cations (X = CH_2, O, and S) appears to be a significant and characteristic fragmentation of these cumulenic ions but not of the isomeric CH_3CNX^{2+} ions.[30]

The neutralization−reionization spectra of these *m*/*z* 121 ions, **8**$^{\bullet+}$ and **9**$^{\bullet+}$ (Figure 2c and d, respectively), feature weak recovery signals and fragmentations similar to those observed in the corresponding CA spectra, except for the absence of the *m*/*z* 93 signal (loss of CH_2N), which is therefore ascribed to a rearrangement process.[31] Similarly, the presence of the recovery signals (R.S.) for the molecular ions is in accord with the molecular orbital calculations (section 5): neutral CH_3CNSe (**8**) is calculated to be a stable species. The absence of charge stripping in the NR spectra is not unprecedented and is due to the lower probability of an m → m^{2+} transition.[32] CH_3CNSe and CH_3NCSe are therefore stable molecules when isolated in the gas phase.

Chemical ionization (**3** as the reagent gas) of benzonitrile and phenyl isocyanide, respectively, generates $PhCNSe^{\bullet+}$ (**2**$^{\bullet+}$)

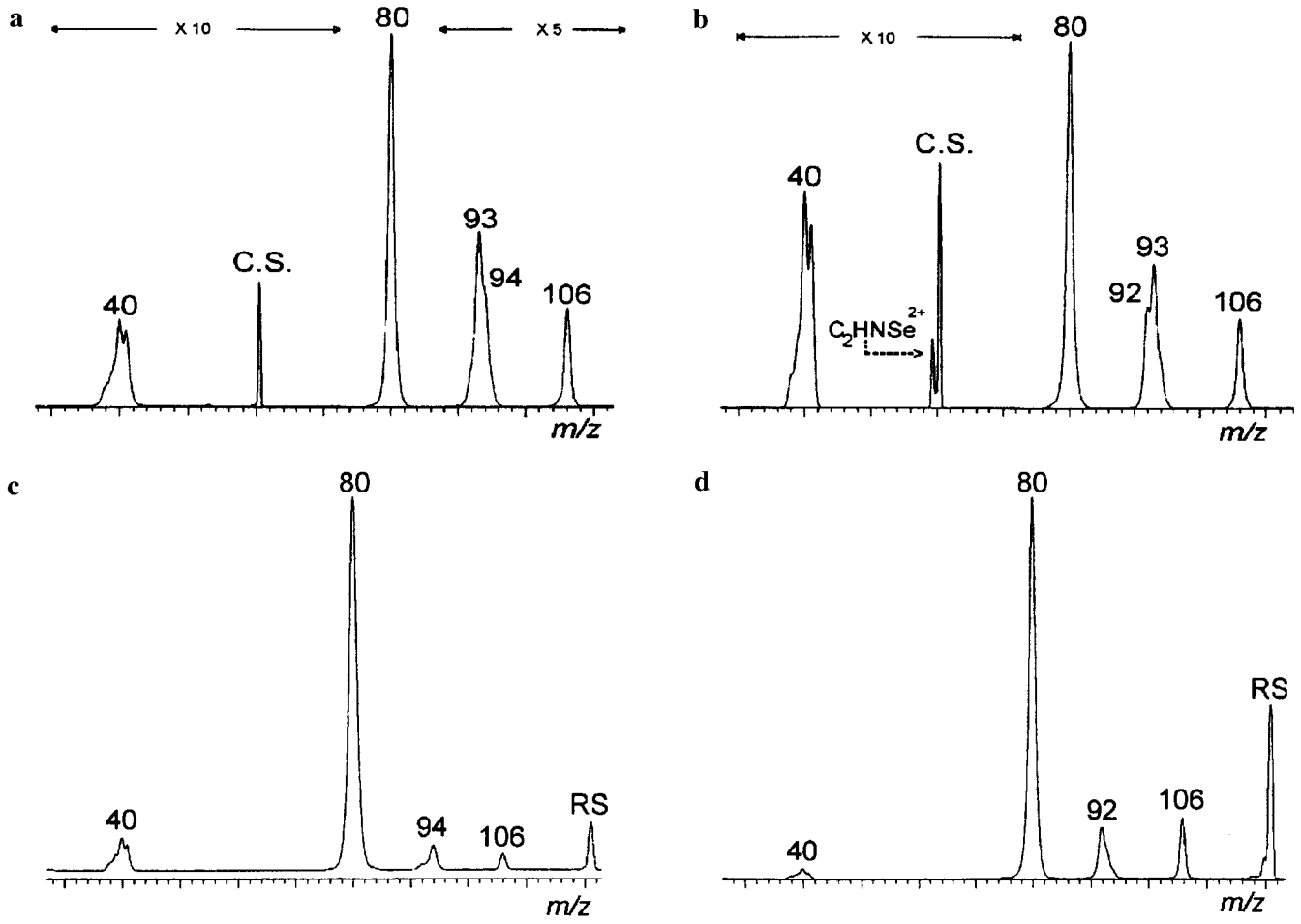

Figure 2. CA (O_2) mass spectra of (a) $CH_3CNSe^{\bullet+}$ and (b) $CH_3NCSe^{\bullet+}$ radical cations (*m*/*z* 121). NR (Xe/O_2) mass spectra of (c) $CH_3CNSe^{\bullet+}$ and (d) $CH_3NCSe^{\bullet+}$ radical cations (*m*/*z* 121) (C.S. = charge stripping). Losses of hydrogen(s) atoms are not shown.

TABLE 3: Collisional Activation Spectra[a] of the Ions Produced by $Se^{\bullet+}$ Transfer to Cyanogen Halides, XCN (X = ^{35}Cl, ^{79}Br, and I)

XCN	X^+	XC^+	$XCN^{\bullet+}$	$Se^{\bullet+}$	NSe^+	$CNSe^+$	C.S.[b]	XSe^+
$[ClCN,Se]^{\bullet+}$	1.5	2	8	100	6	36	8	2.3
11$^{\bullet+}$ (*m*/*z* 141)	(35)	(47)	(61)	(80)	(94)	(106)	(70.5)	(115)
$[BrCN,Se]^{\bullet+}$	2	1	3	100	4	62	11	15
13$^{\bullet+}$ (*m*/*z* 187)	(79)	(91)	(105)	(80)	(94)	(106)	(93.5)	(161)
$[ICN,Se]^{\bullet+}$	100	4.5	25	42	2	63	6	57
15$^{\bullet+}$ (*m*/*z* 233)	(127)	(139)	(153)	(80)	(94)	(106)	(116.5)	(207)

[a] Relative intensities (%), with *m*/*z* values given in parentheses. [b] C.S. = charge stripping.

and $PhNCSe^{\bullet+}$ (**10**$^{\bullet+}$) radical cations. Both connectivities are well characterized by collisional activation. It is worthy of note that there is an important difference between the CA spectrum of **2**$^{\bullet+}$ (R = Ph) and those of **5**$^{\bullet+}$ and **7**$^{\bullet+}$ (R = H) and **8**$^{\bullet+}$ and **9**$^{\bullet+}$ (R = CH_3). The production of $Se^{\bullet+}$ ions is the dominant collision-induced fragmentation when R is H or CH_3, but in the case of R = Ph, the base peak of the CA spectra is associated with the formation of benzonitrile molecular ions. This behavior follows the trend of the ionization energies reported in Table 2.[26] While the CA spectrum of $PhNCSe^{\bullet+}$ (**10**$^{\bullet+}$) radical cations is dominated by the formation of *m*/*z* 77 cations (phenyl cations), the dissociation of the C−Se bond predominantly leads to the generation of phenyl isocyanide radical cations ($PhNC^{\bullet+}$) (Table 2).

Weak but significant recovery signals are present in the NR spectra of **2**$^{\bullet+}$ and **10**$^{\bullet+}$ ions. The base peak of the NR spectrum of $PhCNSe^{\bullet+}$ radical cations corresponds to $Se^{\bullet+}$ ions and is probably due to the reionization of Se atoms lost by collisional activation in the neutralization cell or by spontaneous dissociation of PhCNSe neutrals during their flight between both cells. In recent works, Khuns and Turecek have introduced a new technique to vary neutral lifetimes in NR experiments by using a tandem quadrupole mass spectrometer equipped with an advanced neutralization cell.[18g]

3. $Se^{\bullet+}$ Transfer to Cyanogen Halides and Methyl Thiocyanate. $Se^{\bullet+}$ transfer to cyanogen chloride (ClCN) is also observed upon chemical ionization with **3**. All the collision-induced fragmentations (Table 3), except that leading to *m*/*z* 115 ($ClSe^+$) cations, point to the ClCNSe connectivity (**11**$^{\bullet+}$). Thus, *m*/*z* 106 ($CNSe^+$ cations), *m*/*z* 94 (NSe^+ cations), *m*/*z* 80 ($Se^{\bullet+}$ ions), *m*/*z* 61 ($ClCN^{\bullet+}$ ions), *m*/*z* 47 (ClC^+ cations), and *m*/*z* 35 (Cl^+ ions) can arise from bond cleavages requiring no rearrangement processes. However, the production of the isomeric ions $SeClCN^{\bullet+}$ (**12**$^{\bullet+}$) cannot be excluded, as a significant signal at *m*/*z* 115 ($ClSe^+$ cations) is seen in the CA spectrum. Preliminary experiments have also indicated that alkyl halides are able to trap selenium ions under similar chemical ionization conditions.[29]

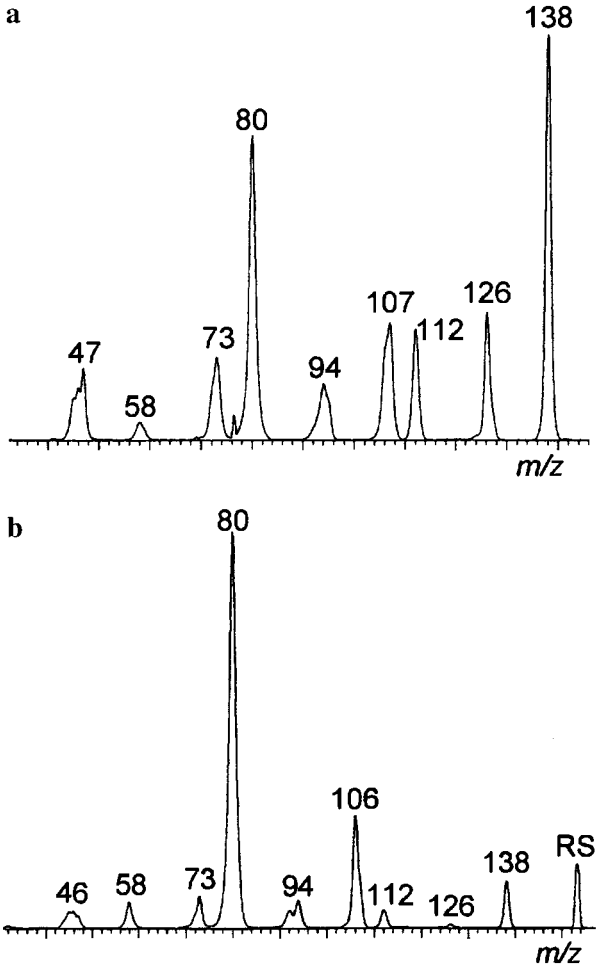

Figure 3. (a) CA (O_2) and (b) NR (Xe/O_2) mass spectrum of *m*/*z* 153 radical cations ($CH_3SCNSe^{\bullet+}$) generated by $Se^{\bullet+}$ transfer to CH_3SCN under CI conditions.

$BrCNSe^{\bullet+}$ radical cations (**13**$^{\bullet+}$) are also readily generated by chemical ionization of BrCN using **3** as the reagent gas. Indeed, the CA spectrum of the so-produced ions (Table 3) is in keeping with the BrCNSe connectivity, the most characteristic peak being *m*/*z* 106 ($CNSe^+$ cations). However, the *m*/*z* 161 signal ($^{79}BrSe^+$ ions) is quite intense and could be explained by the presence of isomeric $SeBrCN^{\bullet+}$ radical cations (**14**$^{\bullet+}$).

Cyanogen iodide (ICN) was studied in a similar manner. The CA spectrum (Table 3) of $[ICN,Se]^{\bullet+}$ ions (*m*/*z* 233) suggests the presence of $ICNSe^{\bullet+}$ ions (**15**$^{\bullet+}$): the strongest peak corresponds to the formation of I^+ and of $CNSe^+$ cations (*m*/*z* 106). The occurrence of an isomeric structure, $SeICN^{\bullet+}$ (**16**$^{\bullet+}$), needs also to be considered, since the signal corresponding to SeI^+ cations (*m*/*z* 207) is very intense in the CA spectrum (Table 3). The intensities of the signals corresponding to the XSe^+ cations steadily decrease in the series ICN, BrCN, and ClCN (Table 3).

Significant recovery signals are observed in all the NR spectra of the **11**$^{\bullet+}$, **13**$^{\bullet+}$, and **15**$^{\bullet+}$ ions, but given the fact that mixtures of isomers are produced, no firm conclusions can be deduced. As suggested by one of the reviewers, an NR/CA experiment on the survivor ions could help in the interpretation. However, for sensitivity reasons, such experiments are not feasible in the present cases.

The CA spectrum (Figure 3a) of $CH_3SCNSe^{\bullet+}$ ions (*m*/*z* 153), generated analogously from methyl thiocyanate (CH_3SCN), is very characteristic of the expected *N*-selenide connectivity CH_3SCNSe (**17**). Most of the fragments are in keeping with this structure: *m*/*z* 138 (loss of $CH_3^{\bullet}$), *m*/*z* 106 ($CNSe^+$ cations), *m*/*z* 94 (NSe^+ cations), *m*/*z* 80 ($Se^{\bullet+}$), *m*/*z* 73 (loss of Se), and *m*/*z* 47 (CH_3S^+ ions). Moreover, the intensities of the *m*/*z* 126 (loss of HCN), *m*/*z* 112 (loss of C_2H_3N), and *m*/*z* 107 (loss of CH_2S) signals, corresponding to fragmentations requiring a rearrangement, are, as expected, of lower relative intensity in the NR spectrum (Figure 3b). This spectrum also features a weak recovery signal. The generation of the cumulenic ions, $S{=}C{=}N^+{=}X$, is the main collision-induced fragmentation of both $CH_3SCNS^{\bullet+}$ (X = S)[17] and $CH_3SCNSe^{\bullet+}$ (X = Se) radical cations.

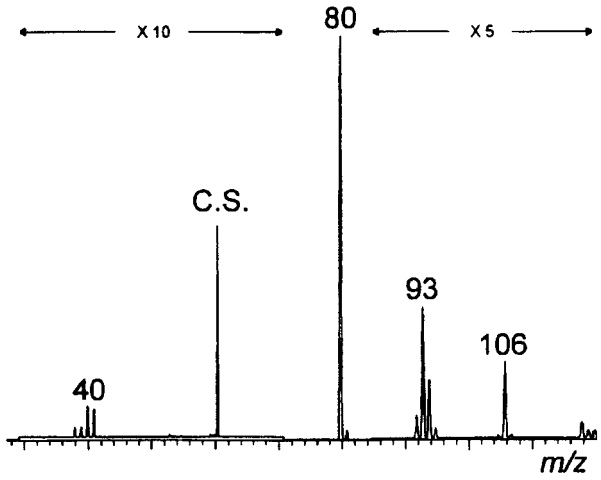

Figure 4. Reaction between mass-selected $NCCNSe^{\bullet+}$ ions and neutral acetonitrile in the Qcell: CA (O_2) spectrum of the mass-selected *m*/*z* 121 ions ($CH_3CNSe^{\bullet+}$) recorded in the linked scan mode (C.S. = charge stripping).

4. Ion−Molecule Reactions Leading to $Se^{\bullet+}$ Transfer. As already mentioned, the $Se^{\bullet+}$ transfer to cyanide groups is the result, in the CI source, of associative ion−molecule reactions. However, the diversity of ionic and neutral species in the ion source prevents the direct determination of the reagent species involved in these reactions. These ambiguities can be removed by using the tandem mass spectrometer in its hybrid configuration.[33] This new arrangement allows the reaction between decelerated mass-selected ions and neutrals in an rf-only quadrupole collision cell (Qcell), the products being detected and characterized after reacceleration (see Experimental Section).

When 3,4-dicyano-1,2,5-selenadiazole molecular ions (**3**$^{\bullet+}$) are allowed to react with neutral acetonitrile in the quadrupole cell, the main products observed arise from decompositions of metastable **3**$^{\bullet+}$ ions yielding $NCCNSe^{\bullet+}$ and $Se^{\bullet+}$ radical cations. However, a closer inspection of the mass spectrum of the produced ions reveals the generation of a small amount of $[CH_3CN,Se]^{\bullet+}$ ions. Mass-selected $Se^{\bullet+}$ also reacts with neutral acetonitrile by $Se^{\bullet+}$ addition, but the yield of the reaction appears to be very low. In contrast, the generation of $CH_3CNSe^{\bullet+}$, (**8**$^{\bullet+}$) is much more significant when the $Se^{\bullet+}$ transfer reaction takes place between mass-selected $NCCNSe^{\bullet+}$ radical cations and neutral CH_3CN. Besides the main beam at *m*/*z* 132 (100%) and the products of metastable fragmentations (*m*/*z* 80, 10%), an intense signal is indeed observed at *m*/*z* 121 (16%).[34] The high kinetic energy (8 keV) CA spectrum of the so-produced ions (Figure 4) is very similar to the CA spectrum of $CH_3CNSe^{\bullet+}$ (**8**$^{\bullet+}$) (Figure 2a) ions (except for the improved resolution in the linked scan experiment). Therefore, the *m*/*z* 121 ions produced in the CI source and in the Qcell must have the same structure. The cyanogen *N*-selenide radical cation is therefore the most efficient reagent for the $Se^{\bullet+}$ transfer reaction.

TABLE 4: Calculated Relative Energies[a] (kJ mol^{-1}) of RCNSe Neutrals

species	relative energy	species	relative energy
HCNSe (**5**)	0.0	NCCNSe (**4**)	0.0
HCN + Se	174.8	NCCN + Se	187.3
HC$^{\bullet}$ + NSe$^{\bullet}$	634.4	CCN$^{\bullet}$ + NSe$^{\bullet}$	566.2
H$^{\bullet}$ + CNSe$^{\bullet}$	319.9	CN$^{\bullet}$ + CNSe$^{\bullet}$	384.7
		N$^{\bullet}$ + CCNSe$^{\bullet}$	984.4
ClCNSe (**11**)	0.0		
ClCN + Se	147.7	CH_3CNSe (**8**)	0.0
ClC$^{\bullet}$ + NSe$^{\bullet}$	446.1	CH_3CN + Se	177.9
Cl$^{\bullet}$ + CNSe$^{\bullet}$	203.2	$CCH_3\bullet$ + NSe$^{\bullet}$	753.5
		$CH_3\bullet$ + CNSe$^{\bullet}$	308.0
BrCNSe (**13**)	0.0	H$^{\bullet}$ + CH_2CNSe$^{\bullet}$	344.4
BrCN + Se	171.7		
BrC$^{\bullet}$ + NSe$^{\bullet}$	485.5	CH_3SCNSe (**17**)	0.0
Br$^{\bullet}$ + CNSe$^{\bullet}$	427.9	CH_3SCN + Se	186.0
		$CH_3SC^{\bullet}$ + NSe$^{\bullet}$	465.2
ICNSe (**15**)	0.0	$CH_3S^{\bullet}$ + CNSe$^{\bullet}$	238.1
ICN + Se	187.0	$CH_3\bullet$ + SCNSe$^{\bullet}$	179.4
IC$^{\bullet}$ + NSe$^{\bullet}$	520.3	H$^{\bullet}$ + $CH_2SCNSe^{\bullet}$	411.5
I$^{\bullet}$ + CNSe$^{\bullet}$	155.9		

[a] G2(MP2,SVP) level. G2(MP2,SVP) E_0 energies include −2585.36093 (NCCNSe), −2493.25519 (HCNSe), −2532.49281 (CH_3CNSe), −2952.37836 (ClCNSe), −5065.25068 (BrCNSe), −2504.18644 (ICNSe), and −2929.93996 (CH_3SCNSe) hartrees.

5. Molecular Orbital Calculations. *Computational Methods*. Standard ab initio[35] and density functional calculations were carried out using the GAUSSIAN92 series of programs.[36] The structures and energies of RCNSe (R = H, CH_3, NH_2, OH, F, Cl, Br, I, CN, and CH_3S) neutrals, RCNSe$^{\bullet+}$ radical cations, and related fragments were examined at the G2(MP2,SVP) level of theory.[37] This corresponds effectively to QCISD(T)/6-311+G(3df,2p)//MP2/6-31G* energies together with zero-point vibrational and isogyric corrections. For iodine, the G2 type basis set has been reported by Radom et al.[38] Spin-restricted calculations were used for closed-shell systems, and spin-unrestricted ones for open-shell systems. The frozen-core approximation was employed for all correlated calculations. Harmonic vibrational frequencies and infrared intensities were computed using the B3-LYP formulation[39] of density functional theory, that is, the Becke's three-parameter exchange functional[39a] and the Lee−Yang−Parr correlation functional.[39b] The directly calculated B3-LYP/6-31G* frequencies were scaled by a factor of 0.9613 to account for the overestimation of calculated frequencies at this level of theory.[40]

Structures and Stabilities of RCNSe Neutrals. All nitrile *N*-selenides are calculated to be thermodynamically stable species (Table 4). In agreement with experimental findings, loss of a selenium atom and loss of the R group are the most favorable dissociation pathways in all cases. The calculated N−Se bond dissociation energies (149−187 kJ mol^{-1}, Table 5) are significantly smaller than those of the corresponding sulfur and oxygen analogues.[17,19] For instance, the N−X bond dissociation energies in the HCNX (X = O, S, and Se) series decrease in the order O > S > Se, being 402, 244 and 175 kJ mol^{-1} (G2(MP2,SVP)), respectively. This suggests that the N−Se bond is the weakest N−X bond in the RCNX series.

We have examined the effect of the substituents on HCNSe by considering the following isodesmic stabilization reaction:[35]

$$RCNSe + CH_4 \rightarrow RCH_3 + HCNSe$$

A positive energy change indicates a relative stabilization effect between the R substituent and the CNSe fragment. The calculated stabilization energies are listed in Table 5. Since the CNSe fragment is both a σ and a π acceptor, it can be stabilized by σ and π donors. The large stabilization by a methyl group can be abscribed to a combination of π (hyperconjugative) and σ donation. The π donor ability decreases in the order NH_2 > OH > F, and the σ acceptor strength increases in the order NH_2 > OH > F. A combination of stabilization by π donation and destabilization by σ acceptance by the substituent leads to the calculated decrease of stabilization energies in the order NH_2 > OH > F. For the halogen substituents, the stabilization energies decrease in the order I > Br > Cl > F, in accordance with the order of σ acceptor strength (or electronegativity). The cyano substituent, being a π acceptor, is calculated to have a destabilizing effect. For the SCH_3 substituent, the positive stabilization is attributed mainly to its σ donating ability.

TABLE 5: Calculated Structural Parameters,[a] Energies, and CN Vibrational Frequencies of RCNSe Neutrals

R	r(R−C)	r(C−N)	r(N−Se)	∠CNSe	ν(CN)[b]	BDE[c]	SE[d]
H	1.067	1.182	1.757	180.0	2082	174.8	0.0
CH_3	1.457	1.180	1.772	180.0	2250	177.9	50.5
NH_2	1.343	1.178	1.788	178.9	2286	171.9	44.6
OH	1.309	1.174	1.770	173.4	2226	156.0	0.1
F	1.309	1.205	1.735	167.5	2110	149.7	−64.4
Cl	1.625	1.186	1.761	178.2	2219	147.7	−34.6
Br	1.776	1.189	1.754	179.8	2218	171.7	−11.0
I	1.990	1.192	1.747	179.0	2155	187.0	8.6
NC	1.351	1.204	1.711	180.0	2127	187.3	−16.3
CH_3S	1.678	1.192	1.753	179.7	2136	186.0	43.7

[a] Bond lengths in angstroms and angles in degrees (MP2/6-31G* values). [b] B3-LYP/6-31G* C≡N stretching frequencies (cm^{-1}), scaled by 0.9613. [c] N−Se Bond dissociation energies (kJ mol^{-1}). [d] Stabilization energies (kJ mol^{-1}): RCNSe + CH_4 → RCH_3 + HCNSe.[40]

TABLE 6: Calculated Relative Energies[a] (kJ mol^{-1}) of HCNSe and HCNSe$^{\bullet+}$

species	neutral	cation
HCNSe	0.0	0.0
1,2-Se shift transition structure	259.0	234.0
selenazirine	24.2	58.8
1,2-H shift transition structure	124.0	253.8
HNCSe	−121.2	−54.1

[a] G2(MP2,SVP) level.

All nitrile *N*-selenides are predicted to have a linear or a slightly bent CNSe structure (Table 5). The calculated C−N bond lengths (1.180−1.204 Å) are somewhat longer than that of a typical C≡N triple bond (e.g. 1.177 Å in HCN, MP2/6-31G*). The calculated N−Se bond length (1.711−1.772 Å) and RCN angle in the nitrile *N*-selenides are strongly influenced by the R substituent. Thus, the N−Se bond lengths in CH_3-CNSe (1.772 Å) and NH_2CNSe (1.788 Å) are rather long while a significantly shorter N−Se bond length (1.711 Å) is calculated for NCCNSe. FCNSe has a relatively short N−Se bond length (1.735 Å) and a significantly bent FCNSe skeleton (∠FCN = 142° and ∠CNSe = 168°). This exceptional structure could be explained in terms of the importance of the R−C^{-}=N^{+}=Se resonance structure. The electron-withdrawing fluorine substituent strongly favors the carbanionic center of the resonance structure. NH_2CNSe and CH_3CNSe are best described by the "normal" R−C≡N^{+}−Se^{-} resonance structure.

We have examined the reaction profile for interconversion of HCNSe to HNCSe using G2(MP2,SVP) theory (Table 6). HCNSe is predicted to lie significantly higher in energy than the isoselenocyanate isomer HNCSe, by 121 kJ mol^{-1}. Interconversion of HCNSe and HNCSe involves a selenazirine

TABLE 7: Calculated Relative Energies[a] (kJ mol^{-1}) of RCNSe$^{\bullet+}$ Radical Cations

species	relative energy	species	relative energy
HCNSe$^{\bullet+}$ (**5**$^{\bullet+}$)	0.0	NCCNSe$^{\bullet+}$ (**4**$^{\bullet+}$)	0.0
HCN + Se$^{\bullet+}$	328.3	NCCN + Se$^{\bullet+}$	263.8
HC$^{\bullet}$ + NSe^{+}	632.7	NCC$^{\bullet}$ + NSe^{+}	487.4
H$^{\bullet}$ + CNSe^{+}	527.4	NC$^{\bullet}$ + CNSe^{+}	515.2
HCN$^{\bullet+}$ + Se	692.9	N$^{\bullet}$ + CCNSe^{+}	882.6
HC^{+} + NSe$^{\bullet}$	828.3	NCCN$^{\bullet+}$ + Se	786.2
H^{+} + CNSe$^{\bullet}$	802.9	NCC^{+} + NSe$^{\bullet}$	744.0
		NC^{+} + CNSe$^{\bullet}$	868.5
ClCNSe$^{\bullet+}$ (**11**$^{\bullet+}$)	0.0	N^{+} + CCNSe$^{\bullet}$	1418.6
ClCN + Se$^{\bullet+}$	348.7		
ClC$^{\bullet}$ + NSe^{+}	491.9	$CH_3CNSe^{\bullet+}$ (**8**$^{\bullet+}$)	0.0
Cl$^{\bullet}$ + CNSe^{+}	458.2	CH_3CN + Se$^{\bullet+}$	390.5
ClCN$^{\bullet+}$ + Se	552.3	$CH_3C^{\bullet}$ + NSe^{+}	810.8
ClC^{+} + NSe$^{\bullet}$	495.0	$CH_3\bullet$ + CNSe^{+}	574.5
Cl^{+} + CNSe$^{\bullet}$	800.9	H$^{\bullet}$ + CH_2CNSe^{+}	342.1
		$CH_3CN^{\bullet+}$ + Se	588.0
BrCNSe$^{\bullet+}$ (**13**$^{\bullet+}$)	0.0	CH_3C^{+} + NSe$^{\bullet}$	644.8
BrCN + Se$^{\bullet+}$	359.9	CH_3+ + CNSe$^{\bullet}$	480.0
BrC$^{\bullet}$ + NSe^{+}	518.4	H^{+} + CH2CNSe$^{\bullet}$	886.5
Br$^{\bullet}$ + CNSe^{+}	669.9		
BrCN$^{\bullet+}$ + Se	525.7	$CH_3SCNSe^{\bullet+}$ (**17**$^{\bullet+}$)	0.0
BrC^{+} + NSe$^{\bullet}$	505.9	CH_3SCN + Se$^{\bullet+}$	417.0
Br^{+} + CNSe$^{\bullet}$	850.5	$CH_3SC^{\bullet}$ + NSe^{+}	541.0
		$CH_3S^{\bullet}$ + CNSe^{+}	523.1
ICNSe$^{\bullet+}$ (**15**$^{\bullet+}$)	0.0	$CH_3\bullet$ + SCNSe^{+}	290.4
ICN + Se$^{\bullet+}$	390.9	H$^{\bullet}$ + CH_2SCNSe^{+}	369.8
IC$^{\bullet}$ + NSe^{+}	563.8	$CH_3SCN^{\bullet+}$ + Se	413.2
I$^{\bullet}$ + CNSe^{+}	408.3	CH_3SC^{+} + NSe$^{\bullet}$	505.7
ICN$^{\bullet+}$ + Se	497.7	CH_3S^{+} + CNSe$^{\bullet}$	441.6
IC^{+} + NSe$^{\bullet}$	512.1	CH_3^{+} + SCNSe$^{\bullet}$	369.9
I^{+} + CNSe$^{\bullet}$	482.6	H^{+} + $CH_2SCNSe^{\bullet}$	972.1

[a] G2(MP2,SVP) level. G2(MP2,SVP) E_0 energies include −2585.01558 (NCCNSe$^{\bullet+}$), −2492.93917 (HCNSe$^{\bullet+}$), −2532.19927 ($CH_3CNSe^{\bullet+}$), −2952.08043 (ClCNSe$^{\bullet+}$), −5064.94784 (BrCNSe$^{\bullet+}$), −2503.88702 (ICNSe$^{\bullet+}$), and −2929.93996 ($CH_3SCNSe^{\bullet+}$) hartrees.

intermediate, which lies 24 kJ mol^{-1} above HCNSe. Rearrangement of HCNSe to this cyclic intermediate, via a 1,2-Se shift transition structure, requires a large activation barrier of 259 kJ mol^{-1}, while rearrangement of the selenazirine to HNCSe, via a 1,2-H shift transition structure, has a smaller barrier of 100 kJ mol^{-1}. Thus, rearrangement of HCNSe to HNCSe is calculated to be a difficult process.

To facilitate future experimental characterization of these cumulenes, calculated B3-LYP/6-31G* C≡N stretching vibrational frequencies are also reported (Table 5). There is a large variation of the cumulenic CNSe stretching frequency, and the magnitude is in accordance with the general trend of the calculated C≡N bond lengths (except for HCNSe): a high CNSe frequency (2286 cm^{-1}) is calculated for NH_2CNSe while a rather low CNSe frequency of 2127 cm^{-1} is predicted for NCCNSe (**4**). For benzonitrile selenide (PhCNSe), the calculated B3-LYP/6-31G* (scaled) CNSe frequency 2213 cm^{-1}, agrees well with the experimental value 2200 cm^{-1}.[20]

Structures and Stabilities of RCNSe$^{\bullet+}$ Radical Cations. Consistent with the experimental findings, all nitrile *N*-selenide radical cations (RCNSe$^{\bullet+}$) are predicted to be stable with respect to all possible fragmentations (Table 7). When fragmentation patterns are compared with calculated energies of fragmentation, it is important to remember that CA spectra consist of the superimposition of collision-induced and unimolecular reactions and that unimolecular fragmentations of metastable ions frequently involve rearrangement processes. It is also worthy of note that the high-energy CA spectra include competitive and consecutive fragmentation reactions. A perfect correlation between observed ion intensities and calculated fragmentation energies is therefore not generally expected. Nevertheless, as found in many cases,[41] the agreement is good.

TABLE 8: Calculated Structural Parameters[a] and Energies of RCNSe$^{\bullet+}$ Radical Cations

R	*r*(R−C)	*r*(C−N)	*r*(N−Se)	∠CNSe	BDE[b]	LUMO[c]
H	1.080	1.148	1.841	180.0	328.3	−3.21
CH_3	1.448	1.161	1.823	180.0	390.5	−2.45
NH_2	1.292	1.179	1.780	180.0	419.8	−1.99
OH	1.263	1.169	1.813	178.1	369.3	−2.75
F	1.243	1.159	1.845	180.0	304.1	−3.21
Cl	1.591	1.162	1.822	180.0	348.7	−2.97
Br	1.745	1.162	1.818	180.0	359.5	−2.94
I	1.971	1.161	1.810	180.0	390.9	−3.51
NC	1.424	1.123	1.857	180.0	263.8	−4.22
CH_3S	1.641	1.178	1.777	179.7	417.7	−2.80

[a] Bond lengths in angstroms and angles in degrees (MP2/6-31G* values). [b] N−Se Bond dissociation energies (kJ mol^{-1}): RCNSe$^{\bullet+}$ → RCN + Se$^{\bullet+}$. [c] LUMO energies (eV), based on HF/6-31G*/MP2/6-31G* wave functions.

The experimental CA spectra of HCNSe$^{\bullet+}$ (**5**$^{\bullet+}$) (Figure 1a) and NCCNSe$^{\bullet+}$ (**4**$^{\bullet+}$)[23] are readily reproduced by theoretical calculations (Table 7). Formation of Se$^{\bullet+}$ (*m*/*z* 80) is the most favorable fragmentation process in both cases. All other peaks agree with predictions.

The calculated fragmentation energies of $CH_3CNSe^{\bullet+}$ (**8**$^{\bullet+}$) are in good accord with the observed CA spectra (Figure 2a). However, the experimental spectrum is complicated by the presence of ions (e.g. peak at *m*/*z* 93) which are due to a rearrangement process.

For ClCNSe$^{\bullet+}$ (**11**$^{\bullet+}$), BrCNSe$^{\bullet+}$ (**13**$^{\bullet+}$), and ICNSe$^{\bullet+}$ (**15**$^{\bullet+}$), the agreement with the observed spectra (Table 3) is reasonably good except for the strong signals due to XSe$^{\bullet+}$ ions, which may be attributed to the presence of the isomeric SeXCN$^{\bullet+}$ ions, as discussed in section 3.

The experimental spectrum of $CH_3SCNSe^{\bullet+}$ (**17**$^{\bullet+}$) (Figure 3a) is also in gross agreement with theoretical expectations except for the strong signals at *m*/*z* 107 (HCNSe$^{\bullet+}$), 112 (SSe$^{\bullet+}$), and 126 (NSSe^{+}), which cannot be formed from unrearranged ions **17**$^{\bullet+}$. The significant reduction of these signals in the NR mass spectrum (Figure 3b) strongly suggests that these ions were formed in rearrangement processes.

All RCNSe$^{\bullet+}$ ions are calculated to have a linear (or almost linear) RCNSe skeleton. Compared to the neutrals, the RCNSe$^{\bullet+}$ radical cations have shorter R−C and C−N bonds but significantly longer N−Se bonds (Table 8). For NCCNSe$^{\bullet+}$, the N−Se equilibrium distance is 0.146 Å longer than that in the neutral! Again, the large variation of N−Se bond lengths correlates well with the calculated N−Se bond dissociation energies (RCNSe$^{\bullet+}$ → RCN + Se$^{\bullet+}$) (Table 8). Interestingly, all RCNSe$^{\bullet+}$ ions are characterized by a low-lying lowest unoccupied molecular orbital (LUMO), −2.0 to −4.2 eV (Table 8).

As with the neutrals, the interconversion of HCNSe$^{\bullet+}$ and HNCSe$^{\bullet+}$ would involve a selenazirine cation intermediate. The 1,2-H shift transition structure lies higher in energy than the 1,2-Se shift transition state on the [HCNSe]$^{\bullet+}$ potential energy surface (Table 6). The overall reaction barrier for rearrangement of HCNSe$^{\bullet+}$ to HNCSe$^{\bullet+}$ is 254 kJ mol^{-1}. Thus, HCNSe$^{\bullet+}$ is confirmed to be a stable species in the gas phase.

RNCSe Neutrals and Radical Cations. As with the oxygen and sulfur analogues, the RCNSe structure is less stable than the RNCSe isomeric structure. However, the relative energies decrease in the order RCNO > RCNS > RCNSe. For example, the calculated HCNX/HNCX relative energies are 271, 155, and 121 kJ mol^{-1} (G2(MP2,SVP)) for X = O, S, and Se,

TABLE 9: Calculated Relative Energies[a] (kJ mol^{-1}) of HNCSe and CH_3NCSe Neutrals and Radical Cations

species	relative energy	species	relative energy
HNCSe (**7**)	0.0	CH_3NCSe (**9**)	0.0
HCNSe	121.2	CH_3CNSe	68.6
HNC + Se	354.4	CH_3NC + Se	343.4
HN + CSe	702.8	CH_3N + CSe	256.2
H$^\bullet$ + NCSe$^\bullet$	337.2	$CH_3\bullet$ + NCSe$^\bullet$	272.7
		H$^\bullet$ + $CH_2NCSe^\bullet$	379.2
$HNCSe^{\bullet+}$ (**7**$^{\bullet+}$)	0.0		
$HCNSe^{\bullet+}$	54.1	$CH_3NCSe^{\bullet+}$ (**9**$^{\bullet+}$)	0.0
HNC + $Se^{\bullet+}$	440.8	$CH_3CNSe^{\bullet+}$	11.2
HN + $CSe^{\bullet+}$	839.6	CH_3NC + $Se^{\bullet+}$	498.7
H$^\bullet$ + $NCSe^+$	512.4	CH_3N + $CSe^{\bullet+}$	461.8
$HNC^{\bullet+}$ + Se	623.5	$CH_3\bullet$ + $NCSe^+$	516.7
$NH^{\bullet+}$ + CSe	921.0	H$^\bullet$ + CH_2NCSe^+	274.7
H^+ + NCSe$^\bullet$	753.1	$CH_3NC^{\bullet+}$ + Se	610.3
		$CH_3N^{\bullet+}$ + CSe	392.4
		CH_3^+ + NCSe$^\bullet$	387.4
		H^+ + $CH_2NCSe^\bullet$	864.0

[a] G2(MP2,SVP) level. G2(MP2,SVP) E_0 energies include −2493.30134 (HNCSe), −2492.95976 ($HNCSe^{\bullet+}$), −2532.51893 (CH_3NCSe), and −2532.20355 ($CH_3NCSe^{\bullet+}$) hartrees.

TABLE 10: Calculated Reaction Enthalpies[a] for $Se^{\bullet+}$ Transfer Reactions[a] of $NCCNSe^{\bullet+}$ to Some Neutrals

reaction	enthalpy	HOMO[b]
HCN + $NCCNSe^{\bullet+}$ → $HCNSe^{\bullet+}$ + NCCN	−64.5	−13.14
FCN + $NCCNSe^{\bullet+}$ → $FCNSe^{\bullet+}$ + NCCN	−26.4	−13.39
ClCN + $NCCNSe^{\bullet+}$ → $ClCNSe^{\bullet+}$ + NCCN	−84.9	−12.52
BrCN + $NCCNSe^{\bullet+}$ → $BrCNSe^{\bullet+}$ + NCCN	−96.1	−12.14
ICN + $NCCNSe^{\bullet+}$ → $ICNSe^{\bullet+}$ + NCCN	−149.0	−11.13
CH_3CN + $NCCNSe^{\bullet+}$ → $CH_3CNSe^{\bullet+}$ + NCCN	−126.7	−12.27
NH_2CN + $NCCNSe^{\bullet+}$ → $NH_2CNSe^{\bullet+}$ + NCCN	−156.0	−11.18
HOCN + $NCCNSe^{\bullet+}$ → $HOCNSe^{\bullet+}$ + NCCN	−105.5	−12.19
CH_3SCN + $NCCNSe^{\bullet+}$ → $CH_3SCNSe^{\bullet+}$ + NCCN	−153.3	−10.37
CH_3Cl + $NCCNSe^{\bullet+}$ → $CH_3ClSe^{\bullet+}$ + NCCN	−35.5	−11.84
CH_3Br + $NCCNSe^{\bullet+}$ → $CH_3BrSe^{\bullet+}$ + NCCN	−71.3	−10.78
CH_3I + $NCCNSe^{\bullet+}$ → $CH_3ISe^{\bullet+}$ + NCCN	−127.3	−9.69
HNC + $NCCNSe^{\bullet+}$ → $HNCSe^{\bullet+}$ + NCCN	−177.1	−13.20
CH_3NC + $NCCNSe^{\bullet+}$ → $CH_3NCSe^{\bullet+}$ + NCCN	−234.9	−12.54

[a] G2(MP2,SVP) values (kJ mol^{-1}). [b] HOMO energies (eV) of neutrals, based on HF/6-31G*//MP2/6-31G* wave functions.

respectively. Both HNCSe and CH_3NCSe are calculated to be thermodynamic stable species, with the homolysis of the N−R bond being calculated to be the most favorable dissociation process. Thus, HNCSe and CH_3NCSe are intrinsically stable species in the gas phase, in conformity with experiment.

As with the neutrals, the $HCNX^{\bullet+}$/$HNCX^{\bullet+}$ relative energies decrease in the order O > S > Se (220, 75, and 54 kJ mol^{-1}, respectively). In the case of the methyl substituent, $CH_3CNSe^{\bullet+}$ is just 11 kJ mol^{-1} less stable than $CH_3NCSe^{\bullet+}$. Both $HNCSe^{\bullet+}$ (**7**$^{\bullet+}$) and $CH_3NCSe^{\bullet+}$ (**9**$^{\bullet+}$) are calculated to be stable species. The computed fragmentation energies (Table 9) are in reasonable accord with the observed CA spectra (Figures 1b and 2b). In agreement with experiment, theory predicts that the loss of a $Se^{\bullet+}$ atom is the most favorable dissociation pathway.

$Se^{\bullet+}$ Transfer Reactions of $NCCNSe^{\bullet+}$. Table 10 summarizes the calculated reaction enthalpies (kJ mol^{-1}) for the $Se^{\bullet+}$ transfer reactions from the $NCCNSe^{\bullet+}$ radical cations (**4**$^{\bullet+}$) to various neutral reagents, nitriles (RCN), isonitriles (RNC), and methyl halides (RCH_3). As one would have expected, the production of isoselenocyanate radical cations starting from isonitriles is more favorable than the $Se^{\bullet+}$ transfer reactions to the corresponding nitriles. Interestingly, the $Se^{\bullet+}$ transfer reactions to methyl halides are also calculated to be exothermic processes, but they are less favorable than the corresponding reactions with nitriles. Therefore, the $Se^{\bullet+}$ transfer reaction to the halogen atom of XCN (X = Cl, Br, and I) is expected to be less favorable than the transfer to the nitrogen atom. These two processes could compete in the case of BrCN and ICN, and such a competition could thus explain the increased intensity of the signals corresponding to XSe^+ cations in the CA spectra (Table 3).

What makes $NCCNSe^{\bullet+}$ an effective $Se^{\bullet+}$ transfer agent? First, we note that $NCCNSe^{\bullet+}$ has a rather low N−Se bond dissociation energy (264 kJ mol^{-1}), the lowest among all the $RCNSe^{\bullet+}$ radical cations considered (Table 8). Second, NC-$CNSe^{\bullet+}$ has a remarkably low LUMO energy (−4.22 eV). For the $Se^{\bullet+}$ transfer reaction, this LUMO could interact favorably with a high-lying HOMO in the neutral reagent. Thus, we would expect the reaction enthalpy to depend on the electron-donating ability (or HOMO energy) of the neutral. Indeed, for each of the three types of neutrals considered, the calculated enthalpies correlate well with their HOMO energies. For nitriles (RCN), the correlation coefficient (r^2) is 0.92. Finally, we note that the positive charge and the unpaired spin in $NCCNSe^{\bullet+}$ are rather localized on the Se atom, in distinct contrast to the case for distonic radical cations. The calculated atomic charge is +0.75 e, on the basis of natural bond orbital (NBO) analysis,[42] and the atomic spin density is 0.99 (on the basis of the HF/6-311+G** wave function).

Conclusions

Nitrile *N*-selenide radical cations, $HCNSe^{\bullet+}$, $CH_3CNSe^{\bullet+}$, $PhCNSe^{\bullet+}$, $ClCNSe^{\bullet+}$, $BrCNSe^{\bullet+}$, $ICNSe^{\bullet+}$, and $CH_3SCNSe^{\bullet+}$, have been generated by the $Se^{\bullet+}$ transfer reaction between $NCCNSe^{\bullet+}$ and nitriles in a new hybrid tandem mass spectrometer. The stabilities of the corresponding neutrals have been investigated by neutralization-reionization and ab initio MO calculations. The neutrals RCNSe are predicted to be observable species in the gas phase, in excellent agreement with the experimental results. However, these neutrals are much less stable with respect to dissociation than the corresponding sulfur and oxygen analogues. All the $RCNSe^{\bullet+}$ cations are predicted to be stable species. Good agreement is observed between calculated and experimentally observed stabilities and fragmentation patterns. $NCCNSe^{\bullet+}$ is found to be an effective $Se^{\bullet+}$ transfer agent because of its low N−Se bond dissociation energy and exceptional low-lying LUMO.

Experimental Section

The spectra were recorded on a large-scale tandem mass spectrometer (Micromass AutoSpec 6F) combining six sectors of EB©E©©EB©E geometry (E stands for electric sector, B for magnetic sector, and © for the collision cells used in this work).[43] General conditions were 8 kV accelerating voltage, 200 μA trap current (in the electron impact mode), 1 mA (in the chemical ionization mode), 70 eV ionizing electron energy, and 200 °C ion source temperature. The solid samples were introduced with a direct insertion probe, while the liquid samples were injected in the ion source via a heated (180 °C) septum inlet.

In the chemical ionization (CI) experiments, 3,4-dicyano-1,2,5-selenadiazole (**3**) was introduced through the direct insertion probe, giving a pressure of about 10^{-5} Torr in the source housing and an estimated pressure of 0.5−1 Torr in the CI cell. The liquid nitrile samples (∼1 mL) were injected into the source via the heated septum inlet. ICN was mixed with **3**

(1:5 ratio), and the mixture was introduced via the direct insertion probe. CA and NR spectra were recorded by scanning the field of the third electric sector and collecting the ions in the fifth field-free region with an off-axis photomultiplier detector.

The installation of an rf-only quadrupole collision cell inside the instrument has been reported elsewhere.[33] Briefly, the experiments utilizing the quadrupole consist of the selection of a beam of fast ions (8 kV) using the first three sectors (EBE), the retardation of these ions to approximately 5 eV, and the reaction with a reagent gas in the cell (the pressure of the reagent gas is estimated to be around 10^{-3} Torr). After reacceleration to 8 kV, all the ions present in the quadrupole cell are separated and mass-measured by scanning the field of the second magnet (B scan). More interestingly, the high-energy CA spectra of the ions present in the quadrupole cell can be recorded by a linked scanning of the fields of the last three sectors (EBE) (resolved mode) or a conventional scanning of the field of the last electric sector after mass selection with the second magnet.

All the samples used were commercially available, except for the selenadiazoles **3** and **6**, whose syntheses are described below.

*3,4-Dicyano-1,2,5-selenadiazole (**3**).*[44] A mixture of diaminomaleonitrile (10.8 g, 0.1 mol) and selenium dioxide (11.2 g, 0.1 mol) in acetonitrile (100 mL) was heated under reflux for 1 h. A small amount of black solid was filtered off, the solvent was removed under reduced pressure, and the residue was chromatographed on silica with dichloromethane to yield 17.7 g (96%). Mp 96−98 °C. MS [*m*/*z* (relative intensity)]: 186-(17.3), 185 (6.8), 184 (100, M, ^{80}Se), 182 (48.7), 132 (70.49). HRMS: 183.9288 (M, ^{80}Se), calculated 183.9288. IR (KBr): 2242 (CN), 1303, 1119, 773, 717 cm^{-1}. ^{13}C NMR ($CDCl_3$): δ 111.51 (CN), 139.49 ppm.

*4-Cyano-1,2,5-selenadiazole-3-carbothioamide (**6**).* A solution of **3** (0.28 g, 1.5 mmol) and thioacetic acid (0.3 g, 4 mmol) in benzene (10 mL) was stirred at ambient temperature for 100 h. The yellow precipitate, which started to appear after about 5 min, was filtered off and triturated on the filter with diethyl ether to yield 0.24 g (73%). Mp >300 °C (decolorized at about 150 °C). MS [*m*/*z* (relative intensity)]: 220 (14.2), 218 (63.05, M, ^{80}Se), 216 (31), 185 (30.3), 183 (14.7), 80 (13), 60 (100). HRMS: 217.9167 (M, ^{80}Se), calculated 217.9165. IR (KBr): 3240 (NH_2), 3148 (NH_2), 2218 (CN), 1591 (C═N), 1427, 1351, 1273, 893, 724 cm^{-1}. ^{1}H NMR (DMSO-d_6): δ 10.01 (1H, s), 10.49 ppm (1H, s). ^{13}C NMR (DMSO-d_6): δ 114.84 (CN), 136.42, 162.81, 190 ppm (C═S).

Acknowledgment. The Mons laboratory thanks the Fonds National de la Recherche Scientifique (FNRS) for its contribution in the acquisition of the large-scale tandem mass spectrometer Micromass AutoSpec 6F and for financial support (P.G.). M.W.W. thanks the National University of Singapore for financial support (Grant no. 970620).

References and Notes

(1) Padwa, A. *1,3-Dipolar Cycloaddition Chemistry;* John Wiley & Sons: New York, 1984; Vols. 1 and 2.

(2) Wentrup, C.; Flammang, R. *J. Phys. Org. Chem.*, in press.

(3) (a) Liebig, J. *Ann. Chim. Phys.* **1823**, *24*, 294. (b) Liebig, J.; Gay-Lussac, J. *Ann. Chim. Phys.* **1824**, *25*, 285. (c) Wöhler, F. *Ann. Chim. Phys.* **1824**, *27*, 196.

(4) For the structures of these acids, see: (a) Hop, C. E. C. A.; van den Berg, K.-J.; Holmes, J. L.; Terlouw, J. K. *J. Am. Chem. Soc*. **1989**, *111*, 72. (b) Teles, J. H.; Maier, G.; Hess, B. E., Jr.; Schaad, L. J.; Winnewisser, M.; Winnewisser, B. P. *Chem. Ber*. **1989**, *122*, 753.

(5) (a) Gasco, A.; Boulton, A. J. *Adv. Heterocycl. Chem.* **1981**, *29*, 252. (b) Pasinszki, T.; Westwood, N. P. C. *J. Chem. Soc., Chem. Commun*. **1995**, 1901. (c) Pasinszki, T. Westwood, N. P. C. *J. Phys. Chem*. **1995**, *99*, 6401.

(6) Maier, G.; Teles, J. H. *Angew. Chem., Int. Ed. Engl*. **1987**, *26*, 155.

(7) (a) Grundmann, C.; Frommeld, H.-D. *J. Org. Chem.* **1966**, *31*, 4235. (b) Kozikowski, A. P.; Adamczyk, M. *J. Org. Chem.* **1983**, *48*, 366.

(8) Flammang, R.; Barbieux-Flammang, M.; Gerbaux, P.; Wentrup, C.; Wong, M. W. *Bull. Soc. Chim. Belg.* **1997**, *106*, 545.

(9) Bertrand, G.; Wentrup, C. *Angew. Chem., Int. Ed. Engl*. **1994**, *33*, 527.

(10) Goldberg, N.; Fiedler, A.; Schwarz, H. *Helv. Chim. Acta* **1994**, *77*, 2354.

(11) Maier, G.; Eckwert, J.; Bothur, A.; Reisenauer, H. P.; Schmidt, C. *Liebigs Ann. Chem.* **1996**, 1041.

(12) (a) Goldberg, N.; Iraqi, M.; Schwarz, H. *Chem. Ber*. **1993**, *126*, 2353. (b) Maier, G.; Schmidt, C.; Reisenauer, H. P.; Endlein, E.; Becker, D.; Eckwert, J.; Hess, B. A.; Schaad, L. J. *Chem. Ber*. **1993**, *126*, 2337.

(13) Stirck, K. M.; Kiminkinen, L. K. M.; Kenttämaa, H. I. *Chem. Rev.* **1992**, *92*, 1649.

(14) (a) Rusli, R. D.; Schwarz, H. *Chem. Ber*. **1990**, *123*, 535. (b) De Koster, C. G.; Van Houte, J. J.; Van Thuijl, J. *Int. J. Mass Spectrom. Ion Processes* **1993**, *123*, 59.

(15) Paton, R. M. *Chem. Soc. Rev.* **1989**, *18*, 33.

(16) Wentrup, C.; Kambouris, P. *Chem. Rev.* **1991**, *91*, 363.

(17) Flammang, R.; Gerbaux, P.; Mørkved, E. H.; Wong, M. W.; Wentrup, C. *J. Phys. Chem.* **1996**, *100*, 17452.

(18) For reviews, see: (a) Wesdemiotis, C.; McLafferty, F. W. *Chem. Rev.* **1987**, *87*, 485. (b) Terlouw, J. K.; Schwarz, H. *Angew. Chem., Int. Ed. Engl.* **1987**, *26*, 205. (c) Holmes, J. L. *Mass Spectrom. Rev.* **1989**, *8*, 513. (d) Flammang, R.; Wentrup, C. *Sulfur Rep.* **1997**, *20*, 255. (e) Goldberg, N.; Schwarz, H. *Acc. Chem. Res.* **1994**, *27*, 347. (f) Schalley, C. A.; Hornung, G.; Schröder, D.; Schwarz, H. *Chem. Soc. Rev.* **1998**, *27*, 91. (g) Khuns, D. W.; Turecek, F. *Org. Mass Spectrom.* **1994**, *29*, 463.

(19) Gerbaux, P.; Flammang, R.; Wong, M. W.; Wentrup, C. *J. Phys. Chem. A* **1997**, *101*, 6970.

(20) (a) Pedersen, C. L.; Harrit, N.; Poliakoff, M.; Dunkin, I. *Acta Chem. Scand.* **1977**, *B31*, 848. (b) Pedersen, C. L.; Hacker, N. *Tetrahedron Lett.* **1977**, *45*, 3981.

(21) (a) Harrit, N.; Holm, A.; Dunkin, I. R.; Poliakoff, M.; Turner, J. J. *J. Chem. Soc., Perkin Trans. 2* **1987**, 1227. (b) Holm, A.; Christiansen, J. J.; Lohse, C. *J. Chem. Soc., Perkin Trans. 1* **1979**, 960.

(22) Poppinger, D.; Radom, L.; Pople, J. A. *J. Am. Chem. Soc.* **1977**, *99*, 7806.

(23) Gerbaux, P.; Flammang, R.; Mørkved, E. V.; Wong, M. W.; Wentrup, C. *Tetrahedron Lett.* **1998**, *39*, 533.

(24) Fehér, M.; Pasinszki, T.; Veszprémi, T. *Inorg. Chem.* **1995**, *34*, 945.

(25) (a) Guo, B.; Pasinszki, T.; Westwood, N. P. C.; Zhang, K.; Bernath, P. F. *J. Chem. Phys.* **1996**, *105*, 4457. (b) Pasinszki, T.; Westwood, N. P. C. *J. Phys. Chem.* **1996**, *100*, 16856.

(26) Lias, S. G.; Bartmess, J. E.; Liebman, J. F.; Holmes, J. L.; Levin, R. D.; Mallard, W. G. *J. Phys. Chem. Ref. Data, Suppl. 1* **1988**, 17.

(27) (a) Jensen, K. A.; Frederiksen, E. *Anorg. Allg. Chem.* **1936**, *230*, 31. (b) Pedersen, C. T. *Acta Chem. Scand.* **1963**, *17*, 1459. (c) Collard-Charon, C.; Renson, M. *Bull. Soc. Chim. Belg.* **1962**, *71*, 531. (d) Henriksen, L.; Ehrbar, U. *Synthesis* **1976**, 519. (e) Barton, D. H. R.; Parekh, S. I.; Tajbakhsh, M.; Theodorakis, E. A.; Tse, C.-L. *Tetrahedron* **1994**, *50*, 639.

(28) Gerbaux, P.; Flammang, R.; Nguyen, M. T.; Salpin, J.-Y.; Bouchoux, G. *J. Phys. Chem. A* **1998**, *102*, 861.

(29) Gerbaux, P.; Flammang, R. Unpublished results.

(30) Further theoretical and experimental work is in progress.

(31) Harnis, D.; Holmes, J. L. *Org. Mass Spectrom.* **1994**, *29*, 213.

(32) Wiedman, F. A.; Cai, J.; Wesdemiotis, C. *Rapid Commun. Mass Spectrom.* **1994**, *8*, 804.

(33) Flammang, R.; Van Haverbeke, Y.; Braybrook, C.; Brown, J. *Rapid Commun. Mass Spectrom.* **1995**, *9*, 795.

(34) It is therefore assumed that the $[CH_3CN, Se]^{\bullet+}$ ions produced during the interaction between $\mathbf{3}^{\bullet+}$ molecular ions and acetonitrile are due to metastably generated $NCCNSe^{\bullet+}$ ions.

(35) Hehre, W. J.; Radom, L.; Schleyer, P. v. R.; Pople, J. A. *Ab Initio Molecular Orbital Theory*; Wiley: New York, 1986.

(36) Frisch, M. J.; Trucks, G. W.; Schlegel, H. B.; Gill, P. M. W.; Johnson, B. G.; Wong, M. W.; Foresman, J. B.; Robb, M. A.; Head-Gordon, M.; Replogle, E. S.; Gomperts, R.; Andres, J. L.; Raghavachari, K.; Binkley, J. S.; Gonzalez, C.; Martin, R. L.; Fox, D. J.; DeFrees, D. J.; Baker, J.; Stewart, J. J. P.; Pople, J. A. *GAUSSIAN92/DFT*; Gaussian Inc.: Pittsburgh, PA, 1992.

(37) (a) Smith, B. J.; Radom, L. *J. Phys. Chem*. **1995**, *99*, 6468. (b) Curtiss, L. A.; Redfern, P. C.; Smith, B. J.; Radom, L. *J. Chem. Phys*. **1996**, *104*, 5148.

(38) Glukhovtsev, M. N.; Pross, A.; McGrath, M. P.; Radom, L. *J. Chem. Phys*. **1996**, *104*, 3407.

(39) (a) Becke, A. D. *J. Chem. Phys.* **1993**, *98*, 5648. (b) Lee, C.; Yang, W.; Parr, R. G. *Phys. Rev. B* **1988**, *37*, 785.

(40) Wong, M. W. *Chem. Phys. Lett*. **1996**, *256*, 391.

(41) For example, see: (a) Flammang, R.; Landu, D.; Laurent, S.; Barbieux-Flammang, M.; Kappe, C. O.; Wong, M. W.; Wentrup, C. *J. Am. Chem. Soc.* **1994**, *116*, 2005. (b) Flammang, R.; Van Haverbeke, Y.; Laurent, S.; Barbieux-Flammang, M.; Wong, M. W.; Wentrup, C. *J. Phys. Chem.* **1994**, *98*, 5801. (c) Wong, M. W.; Flammang, R.; Wentrup, C. *J. Phys. Chem.* **1995**, *99*, 16849.

(42) Reed, A. E.; Curtiss, L. A.; Weinhold, F. *Chem. Rev*. **1988**, *88*, 899.

(43) Bateman, R. H.; Brown, J.; Lefevere, M.; Flammang, R.; Van Haverbeke, Y. *Int. J. Mass Spectrom. Ion Processes* **1992**, *115*, 205.

(44) Shew, D. *Diss. Abstr*. **1959**, 1593.